Behavior of Perforated Metal-to-Composite Joints Subjected to Tensile Loading

Sarah E. Mouring, Ph.D., P.E.
Department of Naval Architecture and Ocean Engineering
United States Naval Academy
Annapolis, USA

Luke Louca, Ph.D., and Reuben Brambleby, M.Sc.
Department of Civil and Environmental Engineering
Imperial College London
London, UK

***Abstract*—Advanced composite materials have many advantages compared to traditional metallic materials including high stiffness- and strength-to-weight ratios, corrosion resistance, damage tolerance, and improved stealth characteristics. Thus, they are being used more often as primary structural members in both civil and military applications. However these materials are not typically applied in isolation due to insufficient stiffness and ductility of composites compared to metallic materials, leading to a rapid expansion of interests in metal and composite combined structures. The design of hybrid metal-to-composite joints is one of the major structural challenges in this area. Hybrid metal-to-composite joints usually entail both material and geometry discontinuities which lead to stiffness mismatch and local stress concentrations. Current research at the U.S. Naval Academy and Imperial College London shows that among the various types of novel metal-to-composite joints, perforated hybrid steel-to-composite joints demonstrate significant potential in naval structural applications. Perforations are cut into the steel increasing the cohesion between steel and composite part of the hybrid joint thus improving the transfer of load between the two parts. In addition to the benefit of mechanical interlocking, it is believed that the perforated steel plate decreases the elastic mismatch between the stiff steel part and the relatively compliant composite part. This paper reviews an Office of Naval Research - sponsored research project focusing on a perforated metal-to-composite joint design subjected to tensile loading.**

Keywords—composite; metal; hybrid; joint.

I. Introduction

Over the last decade there has been a significant move towards lighter and more capable naval vessels. Fiber reinforced polymer (FRP) materials such as glass fiber reinforced polymers (GFRPs) are being more widely used as primary structural members driven by the high demand of advanced naval vessels with enhanced performance in terms of payload, range, stability, corrosion resistance, damage tolerance, stealth, and at the same time, a reduction in lifetime costs. FRP materials have demonstrated that their material properties fulfil the higher performance requirements of these naval applications. A comprehensive review of the potential use of these composite materials for future vessels has been provided by Mouritz,, Geller, Burchill, and Challis [1]. Practice shows that vessels made of FRP can have a greater survivability; however, FRP materials are not typically applied in isolation due to their insufficient stiffness and ductility compared to metallic materials. This has led to quickly growing interests in metal and composite combined structures. However, the susceptibility to failure at the joints in composite structures when subjected to high rate loading from an impulsive load source is one weakness often observed. Thus, one of the major structural challenges appears to be the design of metal-to-composite hybrid joints. Hybrid joints usually entail geometry and material discontinuities which can induce stiffness mismatch and cause local stress concentrations. Also the shock impedance mismatch caused by the different wave propagation characteristics can be crucial to the structural response of the hybrid joints under impulsive loads due to sources such as an air blast or underwater explosion (UNDEX).

Researchers at Imperial College London (ICL) and the U.S. Naval Academy (USNA) have focused recently on characterizing the behavior and ultimate load capacity of metal-to-composite hybrid joints fabricated with different joining methods under various loading conditions. This paper presents initial results from tensile strength testing of steel-to-vinyl ester glass reinforced polymer (GRP) double lap joints, comparing joints that exploit perforated steel plates with those manufactured with non-perforated steel plates and comparing pseudo-static strength with dynamic strength.

II. Background

The concept of applying perforations to the metal part of hybrid joints was first addressed by Unden [2]. The original purpose of the perforations was to increase the cohesion between metal plates and adjacent layers of polymeric material, hence improving the transfer of load between the steel and FRP parts. Also the perforated steel plate was believed to decrease the elastic mismatch between the stiff steel part and the relatively compliant FRP part. This design was further investigated and improved by Melograna and Grenestedt [3] and Cao and Grenestedt [4]. They found that the joint had the highest strength when it was comprised of 7-9 row of circular holes, see Fig. 1. The best performing

U.S. Government work not protected by U.S. Copyright

This is a DRAFT. As such it may not be cited in other works.
The citable Proceedings of the Conference will be published in
IEEE Xplore shortly after the conclusion of the conference.

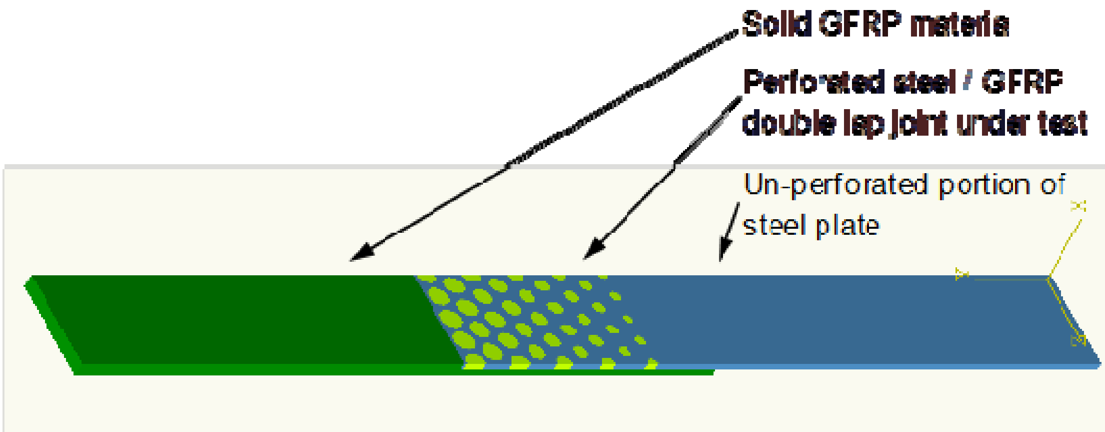

Fig. 1. Half model of the perforated double lap hybrid joint proposed by Melograna and Grenestedt [**3**]

geometry that they tested yielded 25-30% higher tension strength than their non-perforated counterparts. This agrees with Hart-Smith's [5] conclusion that the capacity of hybrid joints can be increased when the joint is detailed such that stiffness imbalance is reduced. It should be noted that most of the recent work has been focused on perforated joints tested under pseudo static loads.

III. Experimental Work

A. Specimen Design

This study is an extension of work reported by Melograna and Grenestedt [3] in which double lap joints between steel and vinyl ester GRP were tested under static loading. The effect of various steel perforation geometries were examined including circular perforations with graduated diameters. The perforations near the tip of the steel plate have the largest diameter and the perforation diameter reduces as distance from the tip of the plate increases, see Figs. 2(a) and 3. A significant effect of this variation in diameter is to gradually increase the effective axial stiffness of the steel plate and thus to mitigate the effects of stiffness mismatch between the GRP and steel materials.

The starting point for the joint design in this study was the design of the strongest joint reported by Melograna and Grenestedt [3]; however, the steel material that was readily available for this study was thinner and of a lower strength than the steel used by Melograna and Grenestedt. Thus a shorter lap length was used here, 40mm rather than 50mm, in order to ensure that failure would occur in the joints themselves rather than in the steel plate beyond the joint. The number of rows of perforations was correspondingly reduced from 9 to 8. The geometry for the remainder of the specimen beyond the joint itself, see Fig. 3, is dictated by the Impact Tension Adapter (ITA) loading device which is described below.

The laminate layup used for the GRP portion of the joints is shown in Fig. 4. TTX1330 is an Owens Corning (OCV) stitched triple ply S2 glass fabric with an overall areal density of 1330 g/m^2. Laminates 1 and 4 become the 40mm long laps which form the joint with the steel plate. The M8610 continuous fiber mat placed at the mid thickness of the layup is provided as a non-structural filler material, permitting laminates 1 and 4 to have a smooth transition onto the steel plate. Two additional layers of TTX1330, laminates 0 and 5, provide the additional thickness required beyond the instrumented portion of the specimen for the ITA bottom clamps.

Intentional fabrication flaws were generated by applying semi-circular pieces of single-sided self-adhesive polytetrafluoroethylene (PTFE) tape to both sides of the steel plate prior to fabrication of the specimen. These flaws are indicated in Fig. 2(b). The materials used for the specimens in this study are given in Table I.

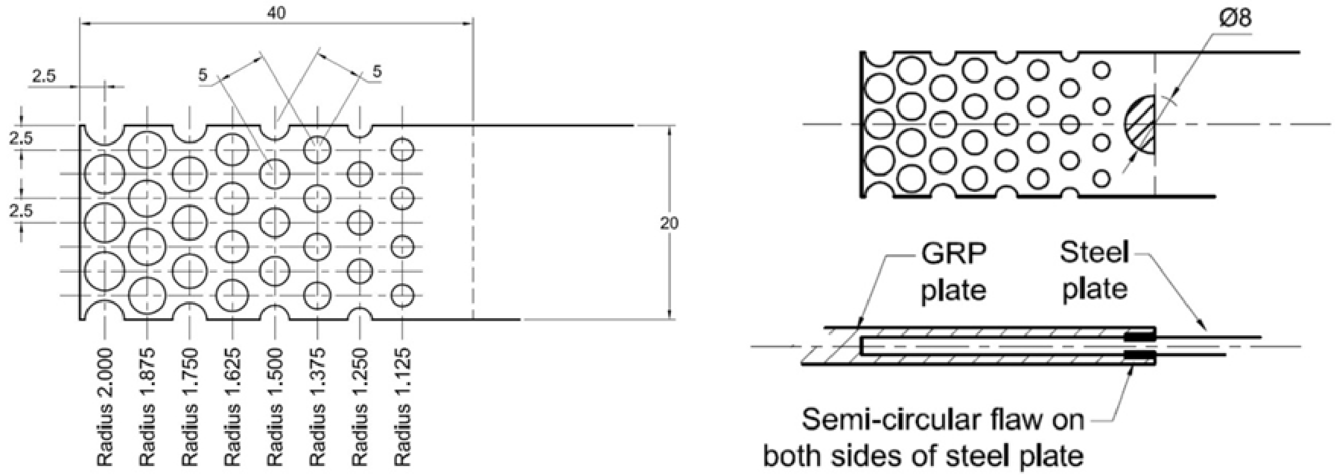

Fig. 2. (a) Perforation geometry (b) Flaw arrangement

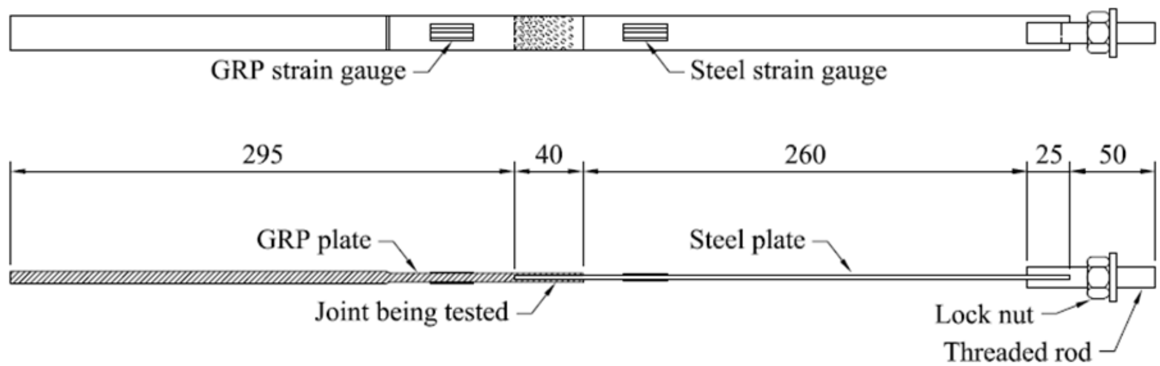

Fig. 3. Overall geometry of the specimens used in this study

TABLE I. MATERIALS USED IN FABRICATION OF JOINT SPECIMENS

Function	Materials Used	Description
GRP Resin	Dow Derakane 510A-40	Epoxy vinyl ester resin
GRP Reinforcement	Owens Corning TTX1330	Stitched glass fabric, +45º, -45º, 0º
GRP Filler	Owens Corning M8610	Glass fiber, continuous filament
Steel Plate	3/32” thick, grade 304	Stainless steel

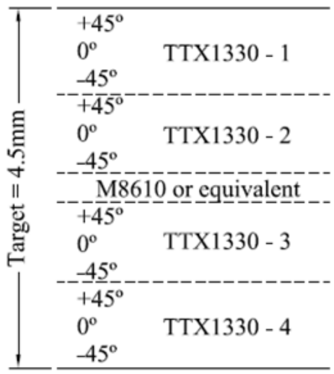

Fig. 4. GRP laminate layup

B. Static Testing

Ten specimens were tested with pseudo-static tensile loading as shown in Table II to determine a baseline strength and baseline failure behavior against which the dynamically loaded specimens can be compared. An Instron uni-axial twin screw test machine fitted with a 2580 series static load cell with a crosshead displacement rate of 1mm/min was used for the pseudo-static tests. In order to measure strain in the GRP plates, strain gauges were applied to the GRP portion of the static specimens beyond the joint itself as shown in Fig. 3. Measurement data was recorded from the strain gauges, the load cell and the crosshead displacement transducer. The data acquisition equipment comprised a Fylde FE-H379-TA high speed transducer amplifier and a windows PC workstation fitted with a high speed data acquisition card. The data acquisition rate for the static testing was 1kHz - the lowest rate available on the card. A specimen ready to be tested under static loading is shown in Fig. 5.

Fig. 5. Specimen in static test rig

TABLE II. SUMMARIZED TEST DETAILS

Static Loading	**Dynamic Loading**
5 Perforated joint specimens 5 Non-perforated joint specimens	6 Perforated joint specimens 6 Non-perforated joint specimens
Screw jack universal test machine Displacement controlled test	Drop weight test machine Impact energy = 44.7 J
1 mm min^{-1} loading rate Steel strain rate ≈ 1x10-4 s^{-1}	Impact velocity ≈ 4.1 m s^{-1} Steel strain rate ≈ 1.4 s^{-1}

C. Dynamic Testing

Twelve specimens were tested under dynamic tensile loading in order to expose differences, in terms of tension strength and failure behavior of the joint, under a higher rate of loading (see Table II). An Instron Dynatup 9200 drop weight test rig was used to generate the dynamic loading. The impact load generated by this rig is converted into a dynamic tension load using the ITA designed and manufactured at ICL. The drop weight mass used in this study was approximately 5.2kg and the impact energy was approximately 45J. Fig. 6 describes the operation of the ITA.

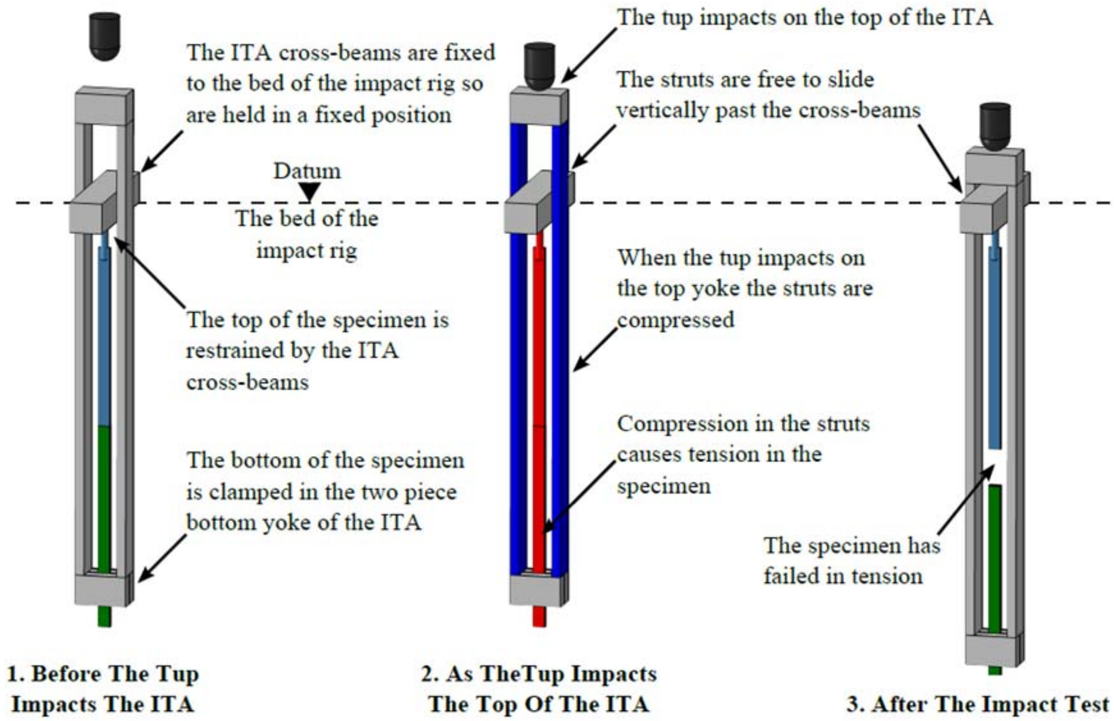

Fig. 6. Operation of the Impact Tension Adapter (ITA)

Strain gauges were applied to both the GRP and steel portions of the specimen as shown in Fig. 3. Measurement data from the strain gauges, impact tup load cell and ITA accelerometer were recorded with a data acquisition rate of 10MHz during the testing. The accelerometer was fixed to the upper surface of the bottom yoke of the ITA. A specimen ready to be tested under dynamic loading is shown in Fig. 7.

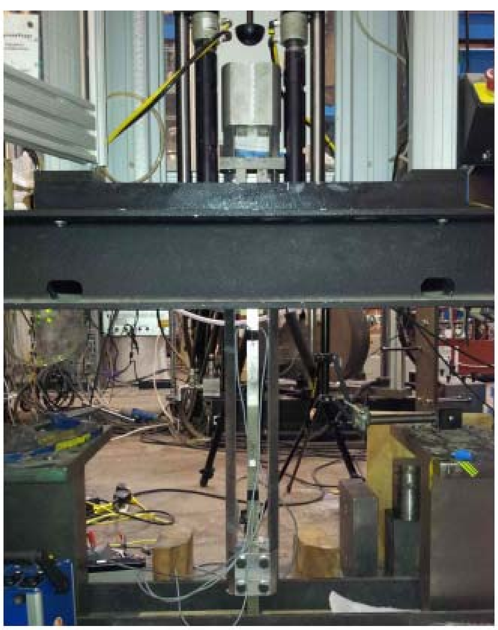

Fig. 7. Specimen in dynamic test rig

D. *Coupon Testing*

In order to determine the strain versus stress relationships for the two materials, tension tests have been carried out for coupons of both the steel and GRP material used in this study. This testing was necessary due to the fact that a load cell was not incorporated into the dynamic test setup. Thus the specimen load must be calculated using the strains measured during the dynamic tests. The pseudo-static coupon tests were carried out at an extension rate of 1mm/min. The averaged results were used to generate polynomial expressions relating strain and stress. These expressions subsequently were used to calculate specimen load from measured strains.

The perforated joints were found to be strong enough to generate significant plastic deformation in the steel plate. The stress strain relationship of the steel is significantly strain rate dependent [6] while the stress strain relationship for the GRP is much less strain rate dependent at the values of strain generated in this study [7]. For this reason the GRP strain measurements are used to calculate the instantaneous joint load in the dynamic tests.

IV. RESULTS AND DISCUSSION

The first round of physical strength testing of both the perforated and non-perforated joints has been completed. Table III gives the mean failure loads from the physical testing. Typical load versus extension plots for static and dynamic loading are given in Fig. 8. The extension is derived from the universal test machine for the static testing; however for the dynamic testing the extension is calculated using data from the accelerometer which is mounted on the bottom yoke of the ITA.

TABLE III. PHYSICAL TEST RESULTS, MEAN FAILURE LOAD IN KN AND SPREAD OF RESULTS (%)

	Static		Dynamic	
Perforated Joint No Flaw	10.8	(±3%)	15.2	(±15%)
Perforated Joint With Flaw	11.0	(±5%)	14.9	(±1%)
Non-perforated Joint No Flaw	4.4	(±56%)	6.2	(±2%)
Non-perforated Joint With Flaw	4.5	(±32%)	6.6	(±6%)

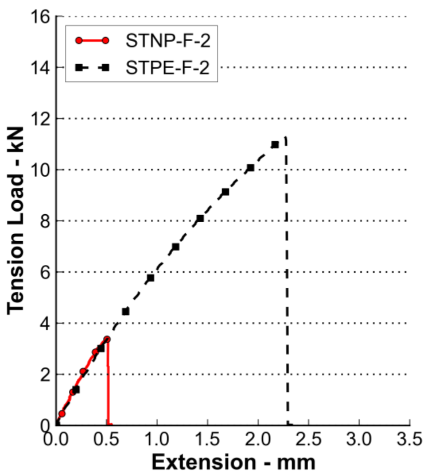

(a.) Static Loading

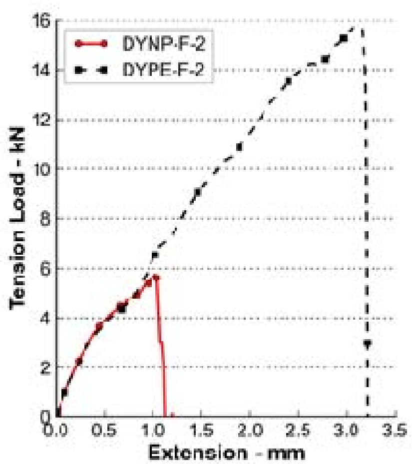

(b.) Dynamic Loading

Fig. 8. Physical test load versus extension plots

Solid line for non-perforated joints, dashed line for perforated joints.

As seen in Fig. 9, there is a relatively clean de-bonding of the GRP from the surface of the non-perforated steel plates when the joint is tested to failure. Some fibers remain bonded to the surface of the steel plates but these are likely to be the stitch yarns of the fabric rather than the actual reinforcing fibers.

Fig. 10 shows the steel plate portion of a tested perforated joint specimen and the gaps that are present between the steel plate perforations and the resin that has penetrated the perforations. These gaps, which are present in all of the tested perforated joints, indicate that the perforated steel plates have undergone plastic deformation prior to failure of the joint.

The results for pseudo-statically loaded joints are qualitatively in agreement with the results reported previously by Melograna and Grenestedt [3], i.e. the perforated joints exhibit significantly greater tension strength than the non-perforated joints. Due to differences in steel surface preparation, steel plate material and steel plate thickness, making a quantitative comparison with the previous results is not particularly meaningful. The results also show that the perforated joints provide an enhancement in strength under dynamic loading.

The perforated joints are stronger than the non-perforated joints by a factor of approximately 2.4 for both static and dynamic loading. The low specification for surface preparation of the steel plates contributes to this dramatic difference in strength. The enhancement under dynamic loading is slightly less, but this difference is small compared to the spread in results data. We could have expected that the strength enhancement under dynamic loading would be lower for the perforated joints due to the fact that plastic softening of the steel will occur at a higher stress as the loading rate increases. The stiffness mitigation effect of the perforations should tend to diminish due to this stiffening of the steel at higher loading rates.

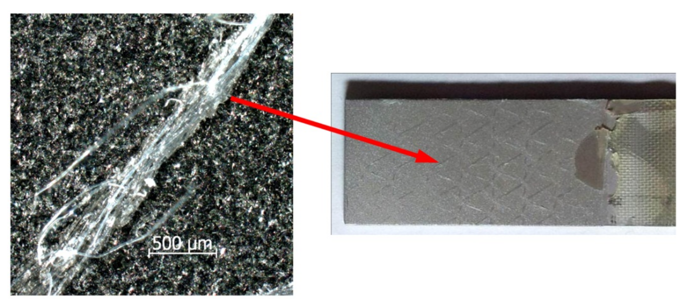

Fig. 9. Steel plate from non-perforated joint specimen

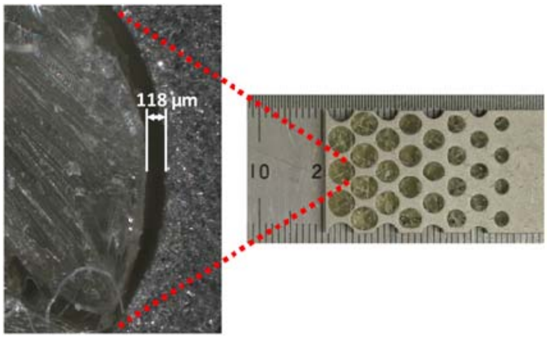

Fig. 10. Evidence of plastic deformation of the steel plate from a perforated joint

Test results also show that the intentional fabrication flaws have little influence on the strength of either type of joint under either type of loading. It is worth noting that the small number of specimens and spread of results may be masking any influence, particularly for the non-perforated joints.

There is a significant enhancement in tension strength under dynamic loading for both perforated and non-perforated joints as shown in Table III. In the dynamic tests strain rates of approximately 1.4 s^{-1} for the steel material and 4.0 s^{-1} for the GRP material beyond the joint itself were generated. Based on data from literature, an increase in tension modulus from these strain rates should be greater for the steel than for the GRP and, as mentioned earlier, an increase in steel stiffness should decrease the strength of the joint, due to an increase in the stiffness mismatch between the two materials. Thus strain rate effects on the adherend materials are not likely to be the source of the increased joint strength under dynamic loads. The more likely source appears to be an enhancement in the cohesive bond between the adherends. Unfortunately there appears to be little consensus in the literature regarding the effect of loading rate on either Mode I or Mode II cohesion for epoxy resins. For example Kusaka et al [8] report that an increase in loading rate leads to a decrease in mode I interlaminar fracture toughness for carbon reinforced epoxy resin; whereas, Carlberger, Biel, and Stigh [9] report that an increase in loading rate leads to an increase in Mode I and a decrease in Mode II fracture toughness for epoxy adhesive.

Finally Figs. 11 and 12 show the GRP strain versus time plot from the dynamic test of a perforated specimen and selected frames from a High Speed Video (HSV) that were captured during the dynamic test of the same specimen. Fig. 12(a) shows an unmodified image; a high pass filter has been applied to the remaining images in Fig. 12 in order to accentuate the damaged area which can be difficult to distinguish in still images. Examining Fig. 12, the failure process for the perforated joint can be described as follows:

- Frame 150 - Just prior to load being applied.
- Frame 206 - De-bond failure initiates at the tip of the steel plate, the darkened area.
- Frame 230 - De-bonding spreads extending in both directions, i.e. along the steel plate and into the solid GRP plate. De-bonding from the steel plate is almost complete, but the bond with the resin in the perforations remains largely intact.
- Frame 236 - The joint has failed; the GRP and steel portions have become separated.

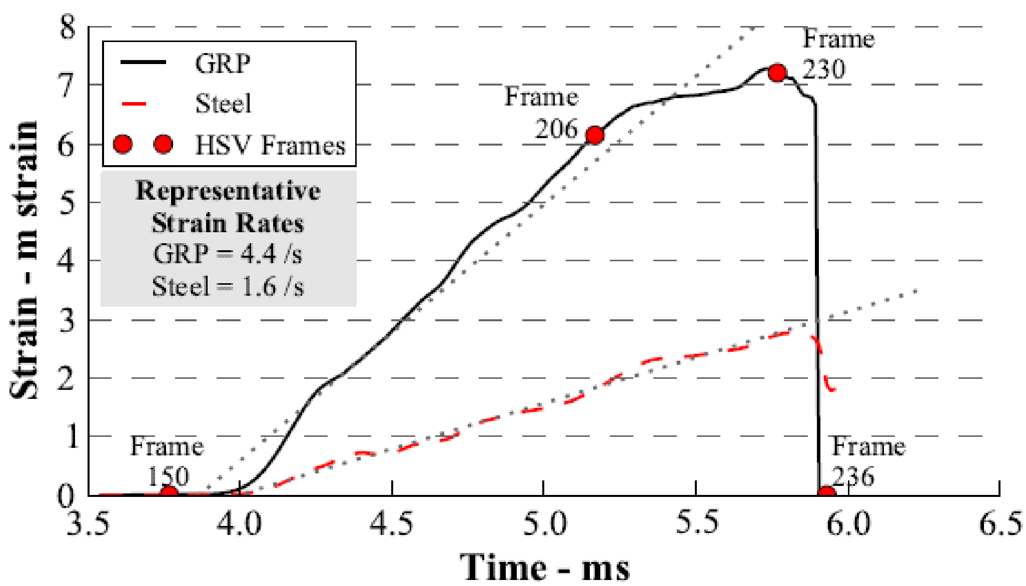

Fig. 11. Strain plot for dynamically loaded perforated joint specimen DYPE-3. The frame numbers relate to the high speed video frames in Fig. 12.

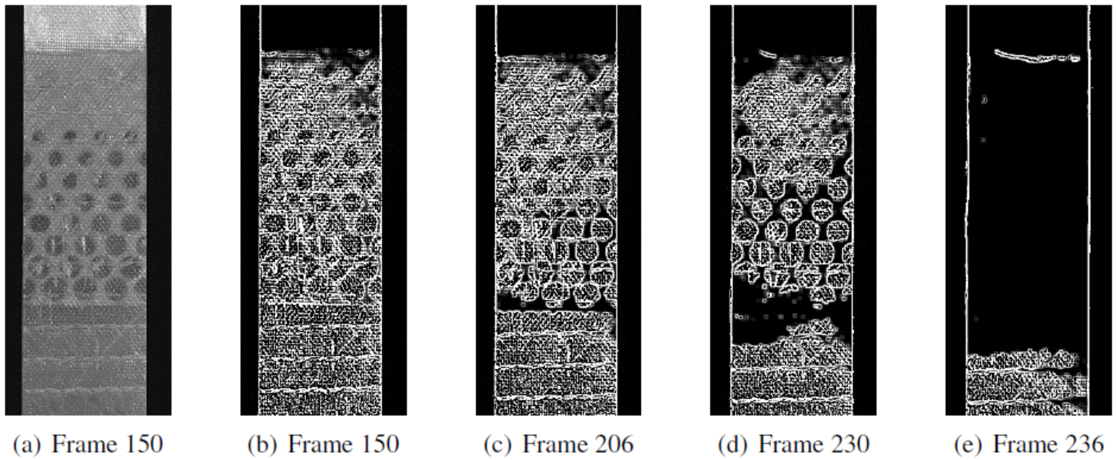

Fig. 12. Individual frames from the high speed video recording of the dynamic test on specimen DYPE-3

V. Conclusions and Future Work

Initial results from tensile strength testing of steel-to-vinyl ester GRP double lap joints, comparing pseudo-static strength with dynamic strength and comparing joints that exploit perforated steel plates with those manufactured with non-perforated steel plates, are presented in this paper. For both perforated and non-perforated joints, an intentional fabrication flaw also was incorporated into half of the joint specimens in order to assess the effect of this flaw type on joint strength. The dynamic tensile loading was applied to the joints using an impact tension adapter designed by the research group at ICL. Both perforated and non-perforated joints were found to be significantly stronger under dynamic tension loads than pseudo-static tension loads. This joint strength increase was slightly less significant for perforated joints than for non-perforated joints.

Future work to determine the origin of the apparent increased joint strength under dynamic loading will include coupon testing of the GRP and steel materials at higher loading rates, Mode II fracture toughness testing for GRP-GRP and GRP-steel interfaces at different loading rates, and Finite Element modeling of the hybrid joints under dynamic tension loading.

Acknowledgment

The authors would like to thank the team at TSD, Project Support Branch, US Naval Academy under the guidance of Mr Doug Loup, Naval Surface Warfare Center Carderock Division for fabricating the specimens used in the experiments, Office of Naval Research for funding the project and Andy Pullen at Imperial College London for his assistance in the experimental work.

References

[1] Mouritz, A.P., Geller, E., Burchill, P., and Challis, K., "Review of advanced composite structures for naval ships and submarines", Composite Structures, 53(1): pp. 21-42, 2001.

[2] Unden, H. and S.-O. Ridder, *Load-introducing armature as component part of a laminated structural element*, 1987.

[3] Melograna, J. D. Grenestedt, J. L., "Improving joints between composites and steel using perforations", Composites: Part A, 33, pp. 1253–1261, 2002.

[4] Cao, J. and J.L. Grenestedt, *Design and testing of joints for composite sandwich/steel hybrid ship hulls.* Composites Part A: Applied Science and Manufacturing, **35**(9): p. 1091-1105, 2004.

[5] Hart-Smith, L.J., *Design of adhesively bonded joints*, in *Joining fibre-reinforced plastics*, F.L. Matthews, Editor. 1987, Elsevier Applied Science: Barking, Essex, England. p. 271 – 311, 1987.

[6] Lichtenfeld, J. A, Tyne, C.J. and Mataya, M. C., "Effect of strain rate on stress strain behavior of alloy 309 and 304l austenitic stainless steel", Metallurgical and Materials Transactions A, 37(1), pp. 147–161, 2006.

[7] Gama, B. A., et al., "High strain-rate behavior of plain-weave s-2 glass/vinyl ester composites", Journal of Composite Materials, 35(13), pp. 1201–1228, 2001.

[8] Kusaka, T., et al., "Rate dependence of mode i fracture behaviour in carbon-fibre/epoxy composite laminates", Composites Science and Technology, 58(3-4), pp.591–602, 1998.

[9] Carlberger, T., Biel, A. and Stigh. U., "Influence of temperature and strain rate on cohesive properties of a structural epoxy adhesive", International Journal of Fracture, 155(2), pp.155–166, 2009.